Journal of Molecular Structure 1300 (2024) 137291

Contents lists available at ScienceDirect

Journal of Molecular Structure

journal homepage: www.elsevier.com/locate/molstr

Novel cinnamic acid-based PET derivatives as quorum sensing modulators

S Skaro Bogojevic [a], D Perminova [b], J Jaksic [b], M Milcic [b], V Medakovic [b], J Milovanovic [a], J Nikodinovic-Runic [a], V Maslak [b,*]

[a] Institute of Molecular Genetics and Genetic Engineering, University of Belgrade, Vojvode Stepe 444a, Belgrade 11000, Serbia
[b] University of Belgrade – Faculty of Chemistry, Studentski trg 12–16, Belgrade 11000, Serbia

ARTICLE INFO

Keywords:
PET derivatives synthesis
Cinnamic acid
Quorum sensing
Molecular docking

ABSTRACT

Poly(ethylene terephthalate) (PET) is widely used material in the healthcare due to its mechanical properties including resistance to chemicals and abrasion. However, it is susceptible to bacterial attachment and contamination. This study addresses some newly designed model compounds of PET with antimicrobial properties that could potentially be incorporated into PET materials. All compounds were synthesized for the first time by labeling an integral part of PET with chromophores in the form of esters of cinnamic and ferulic acids. After complete structural characterization, the effect of new compounds on microbial growth and communication (quorum sensing, QS) was analyzed and further investigated using molecular docking. The obtained results indicate that the introduction of chromophores that have one part of cinnamic acid enriched with a methoxy functional group in them acts as QS modulators. Moreover, compounds exhibited dose-dependent selectivity toward QS signaling pathways and the highest tested concentration of compounds showed *Pseudomonas* Quinolone Signal (PQS) inhibitory activity suggesting that these compounds have a potential effect on pyocyanin production. Docking studies demonstrated that compounds hold binding power to all four QS protein targets (LuxP, periplasmatic protein that binds AI-2 inducer and forms a complex able to transduce the autoinducer signal, RhIR protein that is a key QS transcriptional regulator that activates the genes involved in the synthesis of rhamnolipids and pyocyanin, AbaI protein that has a role in QS signal transduction, and LasR protein which is a key QS transcriptional regulator that activates transcription of genes coding for some virulence-associated traits) while the highest binding strength is observed with compounds 2 and 6 containing single cinnamic acid fragment, suggesting their further biomedical application.

1. Introduction

Bacterial infections represent a major health problem, responsible for great expense and mortality [1]. A significant source of bacterial infections is contaminated and soiled surfaces of indwelling medical devices or common utilities such as sinks, toilets, door handles, clothes, curtains, or computer keyboards [1,2]. Most materials in biomedical applications are replaced with clear, strong, lightweight, and low-cost plastics known as PET [2]. This is one of the most used polymeric materials in the healthcare sector mainly due to its biocompatibility, mechanical strength, and resistance against chemicals [1,3]. Certainly, the main disadvantage of PET use in the healthcare sector is its susceptibility to bacterial contamination. Possible ways to reduce the impact of PET bacterial contamination are the anti-adhesive and biocidal modification of its surfaces [1–4]. Anti-adhesive modification implies surface charge and energy, hydrophilicity, and surface roughness, while biocidal modification may be obtained by attaching antimicrobial compounds to the surface to prevent the growth of bacteria. Modification of PET surface can improve its hemocompatibility and anti-bacterial properties [5,6]. PET is an inert polymer, without surface reactive functional groups, therefore the introduction of reactive functional groups on its surface could improve the desirable properties. In recent years, various techniques as hydrolysis, reduction, and glycolysis, have been applied to the copolymerization and post-modification of oligomers and polymers [1,6–8].

In our previous work, we synthesized several compounds that could be seen either as PET building blocks or as products of PET degradation and assessed their toxicity, and their potential to be used as substrates for PET hydrolyzing enzymes [9]. None of the compounds were affecting the growth of common human pathogens *E. coli* and *S. aureus* even at

* Corresponding author.
E-mail address: vmaslak@chem.bg.ac.rs (V. Maslak).

https://doi.org/10.1016/j.molstruc.2023.137291
Received 21 August 2023; Received in revised form 4 December 2023; Accepted 8 December 2023
Available online 9 December 2023

1000 mg/mL concentrations indicating that compounds do not have any microbial growth inhibitory properties and were not toxic. Therefore, in this study, to improve the antimicrobial properties of the PET model compounds, the labeling of the terephthalic part of PET was achieved using parts of cinnamic and ferulic acids as chromophores (Scheme 1). Cinnamic acid and hydroxycinnamic acids are ubiquitous and their direct extraction from plants and their biotechnological production is the subject of many investigations [10], which is the reason for the increasing popularity of polymers based on cinnamic acid and its derivatives [11,12]. Also, the polymers synthesized from hydroxy derivatives of cinnamic acid are widely applied in biomedicine, especially as drug delivery systems [13]. From a chemical point of view, cinnamic acid has two main characteristics important for its use in polymer synthesis: a conjugated double bond that undergoes *cis-trans* isomerization and provides a possibility of creating photoreactive polymers whose application is found in biomedicine as drug carriers [13], and the presence of hydroxyl and carboxyl groups in its structure enables the polycondensation reactions [13,14]. It is generally known that cinnamic acid can be used as an additive to food-packaging materials and as a savory ingredient in cosmetics and detergents [15–17]. Some studies have shown that cinnamic acid and its derivatives find its potential use in food-packaging applications by obtaining thin materials with starch film, PLA, and PVA, followed by the manifestation of antibacterial activity against *E. coli* and *Listeria innocua* [18–20].

Cinnamic acid derivatives have been reported to have antibacterial, antiviral, and antifungal properties, moreover, some of the cinnamic acid derivatives have been reported as more effective antimicrobial drugs compared to the standard drugs used to treat chronic or infectious diseases in vitro [21,22]. Also, it is known that fungal organisms are generally more susceptible to cinnamic aldehydes, while bacteria are affected by cinnamic acids, esters, and amides [23]. A noteworthy effect was observed for the cinnamic derivatives against *Mycobacterium tuberculosis*. The bacteria growth was repeatedly inhibited by micromolar concentrations of derivatives containing the cinnamic acid moiety [23]. Recently Marina Mingoia et al. reported the synthesis, antimicrobial, antibiofilm, and wound-healing properties of novel cinnamic acid-based antimicrobials [24]. They demonstrated the antimicrobial properties of cinnamic acid-based compounds against Gram-positive bacteria (*Streptococcus* spp.) and antibiofilm activity against *Staphylococcus epidermidis* and proposed it as a safe wound-healing topical agent for the treatment of skin wound infections.

According to our knowledge, to date, there are no reports on cinnamic acid use in the synthesis of PET model compounds as antimicrobials. Therefore, in this study, cinnamic acid-based PET model compounds were synthesized for the first time with the view of incorporation into PET polymers, and their bioactivity has been determined indicating their ability to inhibit bacterial communication (quorum sensing).

2. Material and methods

2.1. Materials

Ethanol (CAS No.: 64-17-5), methanol (CAS No.: 67-56-1), dimethyl sulfoxide (DMSO; CAS No.: 67-68-5), deuterated DMSO (CAS No.: 2206-27-1), methyl terephthaloyl chloride (CAS No.: 100-20-9), terephthalic acid (CAS No.: 100-21-0), hydroxycinnamic acid (CAS No..: 14755-02-3), concentrated sulfuric acid (CAS No.: 7664-93-9), anhydrous sodium sulfate (CAS No.: 7757-82-6), sodium bicarbonate (CAS No.: 144-55-8), pyridine (CAS No.: 110-86-1), potassium hydroxide (CAS No.: 1310-58-3), dicyclohexylcarbo-diimide (DCC; CAS No.: 538-75-0) and 4-dimethylaminopyridine (DMAP; CAS No.: 1122-58-3) were obtained from Sigma-Aldrich (St. Louis, Missouri, USA).

2.2. Synthesis of PET derivatives

All reactions were performed using previously purified reagents and solvents following standard purification techniques. The reactions were monitored by thin-layer chromatography (TLC), on 0.25 mm plates (Merck (60F-254) and 18–34,60 Å, ICN Silica TLC), UV light, solution of *p*-anisaldehyde in ethanol (PAA), as well as 50% sulfuric acid solution with subsequent heating of the plate, were used to visualize the spots. Chromatographic purifications were performed using dry-flash chromatography (silica-gel 10–18, 60 Å, ICN Biomedicals). NMR spectra were recorded on a Varian/Agilent instrument (^{1}H NMR at 400 MHz, ^{13}C NMR at 100 MHz). Chemical shifts are expressed in ppm (δ), using tetramethyl silane (TMS) as the internal standard, while coupling constants (*J*) are expressed in hertz (Hz). IR spectra were recorded on a NICOLET SUMMIT instrument, frequencies are expressed in cm^{-1}.

Model compounds **1–6** (Fig. 1.) were synthesized according to the general procedures for the preparation of different esters by reaction of alcohols with a) acyl chloride in the presence of a base, and b) with carboxylic acids in the presence of DCC. Detailed synthetic procedures are explained in the supporting material, chemistry part. Briefly, PET model compounds **1, 2, 3,** and **4** were prepared by reaction of appropriate esters with methyl terephthaloyl chloride or terephthaloyl dichloride in the presence of a base at room temperature. While, model compounds **5** and **6** were obtained by the reaction of the terephthalic acid derivative with the hydroxycinnamic and ferulic acid derivatives in the presence of carboxyl group activators in the form of DCC (N,N'-Dicyclohexylcarbodiimide) and DMAP (4-Dimethylaminopyridine).

2.3. Antimicrobial tests

Minimum Inhibitory Concentration (MIC) values of samples were determined according to the standard broth micro-dilution assays, following the Standards of the European Committee on Antimicrobial

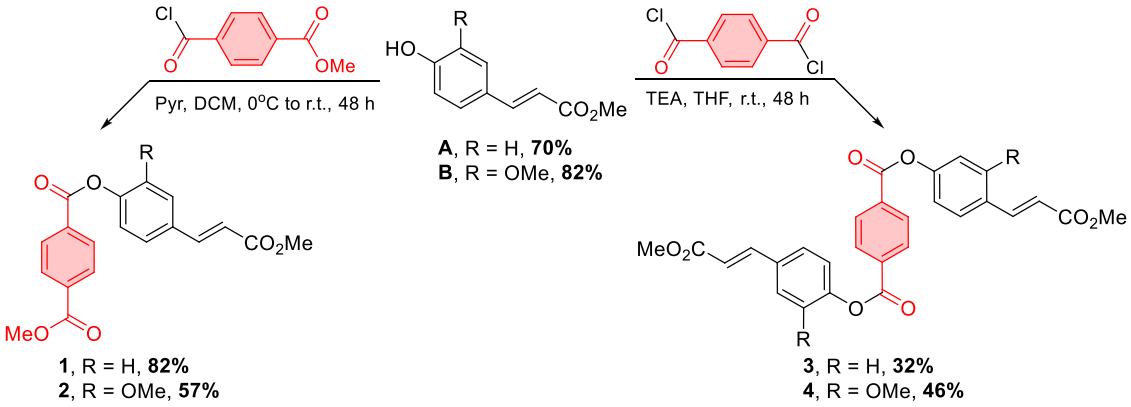

Scheme 1. Routs of the synthesis of PET model compounds (red = terephthaloyl part of PET, blue = ethylene glycolic part of PET).

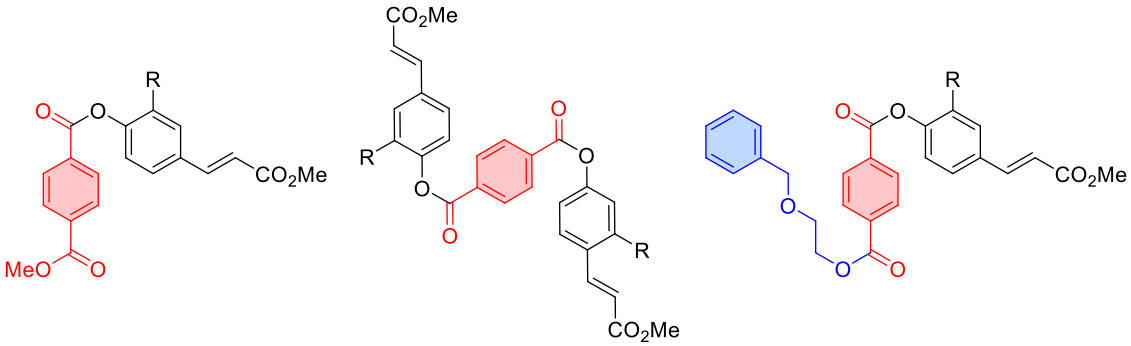

Fig. 1. Schematic presentation of six novels synthesized PET model compounds (red = terephthaloyl part of PET, blue = ethylene glycolic part of PET).

Susceptibility Testing (v 7.3.1: Method for the determination of broth dilution minimum inhibitory concentrations of antifungal agents for yeasts) for *Candida* spp., and according to the standard broth microdilution assays, recommended by the National Committee for Clinical Laboratory Standards (M07-A8) for bacteria. The tested compounds were dissolved in DMSO at a concentration of 50 mg/mL. The highest concentration used was 250 μg/mL. *Candida* strain used in this study was *Candida albicans* ATCC 10231 and *Candida parapsilosis* ATCC 22019, and bacterial strains included: Staphylococcus aureus ATCC 25923, *Escherichia coli* NCTC 9001, *Pseudomonas aeruginosa* NCTC 10662. For the MIC assessment, the inoculums were 1×10^5 colony-forming units (CFU/mL), for *Candida* species, and for bacteria 5×10^5 colony-forming units (CFU/mL). The MIC value was recorded as the lowest concentration that inhibited the growth after 24 h at 37 °C.

2.4. Quorum sensing inhibition assays

Chromobacterium violaceum Cv026 violacein inhibition assay. Chromobacterium violaceum Cv026 was used for the assessment of the violacein production controlled by quorum sensing. This strain was cultivated overnight at 30 °C and 180 rpm. Into semi-solid LB agar (0.3 %, w/v, 5 mL) 50 μL of an overnight culture of *C. violaceum* Cv026 was seeded and supplemented with N-hexanoyl-l-homoserine lactone (Sigma, Germany, CAS Number: 147795-39-9) to a final concentration of 5 μM and it was poured over the surface of LB agar plates. After solidification, the sterile discs were placed on the surface of the plates and the tested compounds were added in appropriate concentrations (250 and 500 μg/mL). Petri dishes were incubated at 30 °C in an upright position overnight. Inhibition of violacein production was defined as the presence of blurry white hallows around discs containing active compounds.

Serratia marcescens ATCC 27117 prodigiosin inhibition assay. S. marcescens inoculum was grown in Luria Bertani (LB) broth on a rotary shaker at 180 rpm overnight and the next day the culture was diluted 100-fold in molten semisolid LB agar (0.3 % w/v) and poured over a solid LB medium. Cellulose disks containing compounds (250 and 500 μg/disk) were placed on solidified agar and incubated for 24 h at 30 °C. Inhibition of prodigiosin synthesis was identified by the absence of red color around the disk.

Pseudomonas QS pathways using biosensor strains. Three *Pseudomonas aeruginosa* biosensor strains were used for this assay, *P. aeruginosa* PA14-R3 (ΔlasI Prsal::lux) [25], PAOJP2/pKD-rhlA (ΔrhlA PrhlA::lux) [26] and *P. aeruginosa* PAO1 ΔpqsA (CTX lux::pqsA) [27]. Biosensor strains were cultivated overnight, afterward diluted to OD_{600} 0.045, and incubated with PET compounds in six different concentrations (250 μg/mL, 125 μg/mL, 62.5 μg/mL, 31.2 μg/mL, 15.6 μg/mL, 7.8 μg/mL) in the presence of autoinducers, each specific for its biosensor strain (3OC12HSL, C4-HSL, and HHQ respectively) in a final concentration of 5 μM. Plates were incubated for 4 h, at 37 °C on a rotary shaker at 70 rpm. Cell density (OD_{600}) and bioluminescence (LCPS) were measured after incubation using a Tecan Infinite200 multiplate-reader (Tecan Group Ltd., Switzerland). Luminescence values were normalized per cell density.

2.5. Molecular docking

In the docking experiment, the binding of investigated PET model compounds to the four most studied QS protein targets were investigated. The structures of LuxP and LasR proteins were obtained from Protein Data Bank (PDB ID: 1JX6 [28] and 6MVN [29]), while the structures of AbaI and RhlR proteins (not found in PDB) were modeled as homology models from Swiss-model repository (https://swissmodel.expasy.org/repository/uniprot/B0FLN1 [30] and https://swissmodel.expasy.org/repository/uniprot/ P54292 [31]). The validation of the modeled protein structures was done by stereochemical examination of Ramachandran plots with the PROCHECK [32] program, global Qualitative Model Energy Analysis (QMEANDisCo) scoring function [33], and Protein Structure Analysis Server (ProSA) [34]. Non-bonded atom-atom interactions in the modeled structures (compared to a database of reliable high-resolution structures) were verified by the ERRAT [35] program from the SAVES server [36]. The results of the validation have shown the good overall quality of the modeled protein structures (Figures S9-S16), thus, models of Abal and RhlR proteins were included in our docking experiment.

For all investigated proteins, the H++ program [37], based on the finite difference Poisson–Boltzmann (FDPB) continuum electrostatics method, was used to determine the protonation state of each titratable amino acid. Next, protein structures were relaxed by optimizing for 5000 optimization steps with the program CHARMM using the charmm36 force field [38]. Finally, individual atomic Kollman charges (total charge: −7.908 for LuxP, −1.946 for Abal, −5.944 for LasR, and −0.929 for RhlR) and standard residue atom types, needed for the docking calculations, were added [36,39] to the optimized protein geometries with the AutoDockTools program [40]. The structures of investigated PET model compounds were obtained by fully optimizing initial geometries with B3LYP [41,42]method and 6-311G(d,p) basis set in the Gaussian09 program package [43]. AutoDockTools [40] program was used to add atom types and individual Gasteiger partial charges to PET model compound atoms (total charge: −0.003 for compound 1, −0.003 for compound 2, −0.002 for compound 3, −0.002 for compound 4, −0.001 for compound 5 and −0.001 for compound 6) and define rotatable bonds (8 for compound 1, 9 for compound 2, 12 for compound 3, 14 for compound 4, 13 for compound 5 and 14 for compound 6) and prepare .pdbqt files for docking experiment.

The docking experiments were carried out with two different docking programs: AutoDock 4 [44] and the Auto-Dock Vina program [45], using different search algorithms and scoring functions. For ligands, all double bonds were kept rigid in Z-conformation, while all single bonds

were set to rotate freely during calculation. The blind docking experiment with the AutoDock4 program was conducted in one large grid box, centered at the center of the protein, with a spacing of 0.375 Å between individual grid points. The dimensions of the grids were: 51 Å × 58.5 Å × 66 Å for LuxP protein; 51 Å × 54 Å × 43.5 Å for AbaI protein; 48 Å × 42 Å × 36 Å for LasR and 45.75 Å × 58.5 Å × 70.5 Å for RhlR protein. The 100 runs of Lamarckian Genetic Algorithm with 150 individuals in population, 25,000,000 energy evaluations, and 27,000 number of generations were employed for each docking run. Every docking run was repeated three times and the average binding energy for the best docking pose was reported.

A different blind docking strategy was employed for the docking experiment with the AutoDock Vina program. To increase our chances of finding the best ligand binding sites, docking was done in a smaller grid box which was stepwise moved for 8 Å in one direction at a time until the whole surface and volume of the protein was covered. To cover the whole surface and volume of LuxP protein a total of 448 small grid boxes were constructed and the same number of docking runs were produced for every ligand. For AbaI protein 294 grid boxes was needed, 252 grid boxes for LasR, and 504 grid boxes for RlhR protein. The size of these small grid boxes was set to allow for full conformational freedom of the ligand. For smaller compounds 1 and 2 the size of the grid box was 26 × 26 × 26 Å. and for the larger compounds 3, 4, 5, and 6 the size of the grid box was 34 × 34 × 34 Å. The exhaustiveness parameter was set to 50 in each docking run. This large number of smaller grid boxes docking approach has given us a good result in our previous investigations [46, 47]. Discovery Studio software [48] was used to analyze and visualize the results of the docking study.

3. Results and discussion

3.1. Chemistry

In our studies, the synthesis of the desired PET model compounds started with a simple esterification reaction of the hydroxycinnamic acid under acidic conditions (Scheme 1., compounds **A** and **B**) [49]. PET model compounds with one chromophore unit were prepared by reaction of the appropriate methyl ester of 4-hydroxycinnamic acid with methyl terephthaloyl chloride in the presence of pyridine as a base (Scheme 1., compounds **1** and **2**), while, on the other side, PET model compounds with two chromophore units were obtained by reaction of hydroxy esters and terephthaloyl chloride in the presence of triethylamine as a base (Scheme 1., compounds **3** and **4**).

A challenge in the synthesis was the functionalization of the 4-((2-(benzyloxy)ethoxy)carbonyl)benzoic acid PET monomer with methyl esters of hydroxycinnamic and ferulic acids. The starting material was prepared according to the previously described procedure [9]. Model compounds **5** and **6** were obtained according to the Steglich procedure for the preparation of esters by reaction of carboxylic acids with methyl esters of hydroxycinnamic acid **A** and **B** in the presence of DCC and DMAP (Scheme 2).

It is of great importance to note that model compounds were prepared and characterized for the first time. Therefore, for all compounds, the solubility in solvents of different polarities was tested (**Table S1**). Seven solvents of different polarities were used to test the compound solubility: toluene, chloroform, acetonitrile, ethyl acetate, dimethyl sulfoxide, methanol, and water. As can be seen from **Table S1**, all compounds showed similar and very good solubility in chloroform, except for derivatives of terephthalic acid, **3** and **4,** with two chromophores, which shows very poor solubility in all tested solvents. Also, the good solubility of most compounds can be observed in dimethyl sulfoxide, while water proved to be a poor solvent for all compounds. Compound **2** and compound **6** showed the best solubilities in all tested solvents, except water.

3.2. Antimicrobial activity

Poly(ethylene terephthalate) is powerless against microbial contamination, which poses a threat to human health. Thus, endowing PET with an anti-adhesion surface, but without releasing germicide, is currently still a challenge. To address this issue, a lot of research was done on changing PET surfaces [1–4].

The antimicrobial activity of cinnamic acid and cinnamaldehyde for bacterial growth control was demonstrated [50,51]. Cinnamaldehyde was able to inhibit planktonic growth at low concentrations but almost all cinnamic acid derivatives affected bacterial growth parameters in *E. coli, S. aureus, and E. hiraei* (doubling time, and lag phase length) [51]. Therefore, in our study, we tested compounds for their antifungal and antibacterial effects. For the initial biological assessment, we analyzed our PET compounds (**1–6**) in terms of antimicrobial properties against *C. albicans* ATCC 10231, *C. parapsilosis* ATCC 22019, *E. coli* NCTC 9001, *S. aureus* ATCC 25923, and *P. aeruginosa* NCTC 10662. The antimicrobial activities of the compounds were determined as their minimal inhibitory concentrations (MICs) and reported in (**Table S2**). None of the tested compounds had an impact on the growth of any of the tested strains, i.e., MIC-values of over 250 μg/mL were observed. According to the obtained

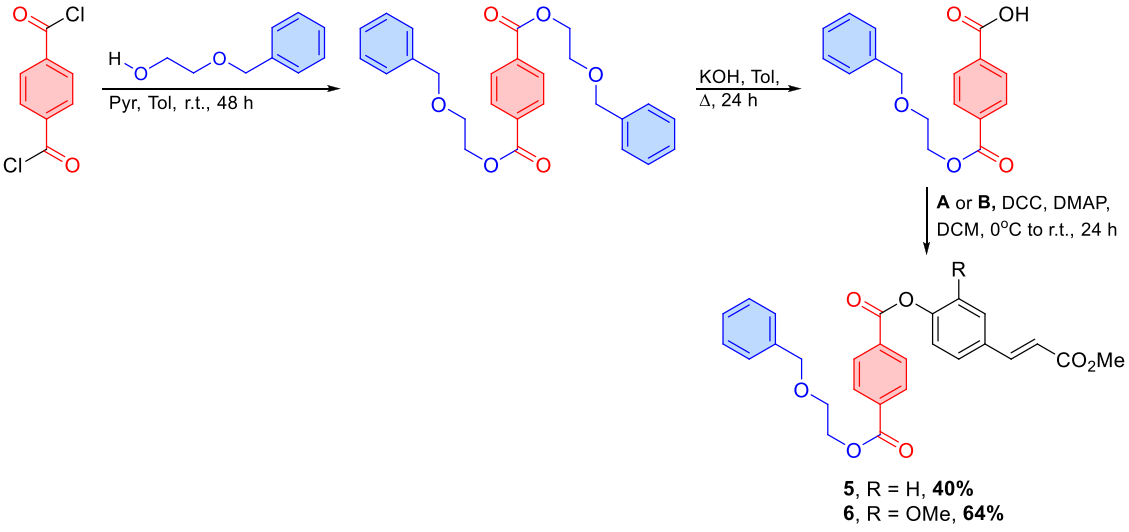

Scheme 2. The functionalization of the 4-((2-(benzyloxy)ethoxy)carbonyl)benzoic acid, PET monomer, with methyl esters of hydroxycinnamic acid **A** and **B** (red = terephthaloyl part of PET, blue = ethylene glycolic part of PET).

results, we decided to test if our model compounds could modulate bacterial intercellular communication by affecting QS pathways. In brief, QS is a way of communication between bacteria of the same or different species through signaling molecules. QS systems control pathogenesis by regulating the expression of virulence determinants [52]. Therefore, for the development of antimicrobial therapeutical products that deal with bacterial virulence, the initiation of QS inhibitors without affecting the growth and survival of pathogenic bacteria is of great interest. In this work, initial QS screening was done using *C. violaceum* Cv026 and *S. marcescence* ATCC 27117 for the inhibition of the violacein or prodigiosin production, respectively, which are under QS control [53,54]. It was found that the quorum-dependent production of violacein and prodigiosin was inhibited to different degrees in the presence of the test compounds. Mild to moderate inhibitory activity was observed with compound **6** visible like a blurry white halo, with a diameter of 1 cm around the disc in a concentration of 250 μg/disc, and compound **4** represented light prodigiosin inhibition (**Fig. S1**). The rest of the test compounds **1, 2, 3**, and **5**, showed less or no activities. What can be taken into consideration based on the obtained results is that a compound possessing only one methylated cinnamic acid fragment (compound **6**) has a potential effect on the QS pathway in both tested bacteria, which is in line with the results of Jantaruk et al. (2021) research [55]. They found that the methyl keto analogue of the corresponding cinnamic acid inhibits QS-controlled violacein production of *C. violaceum* ATCC12472, the inhibitory activity was approximately twofold stronger than the activity of the "parent" cinnamic acid.

To examine in more detail the potential impact of the **1–6** PET model compounds on the QS pathway we tried to identify which of the signaling pathways were affected. Therefore, we evaluated their ability to bind to QS receptors in the presence of exogenously provided autoinducers using *P. aeruginosa* biosensors designed to differentiate QS pathways: *P. aeruginosa* PA14-R3 (ΔlasI Prsal::lux) [25], *P. aeruginosa* PAOJP2/pKD-rhlA (ΔrhlA PrhlA::lux) [26] and *P. aeruginosa* PAO1 ΔpqsA (CTX lux::pqsA) [27]. *P. aeruginosa* is an intensively studied bacterium owing to multidrug resistance and biofilm-forming ability like a major health problem [56]. The remarkable ability of *P. aeruginosa* to efficiently adhere to surfaces and form long-lasting biofilms promotes chronic infectious diseases [56].

In the highest tested concentration, 250 μg/mL, only compounds: **2** and **6** showed inhibition effects on all three biosensors (Table 1), while in a lower concentration, just compound **6** showed a significant inhibition effect on the R3 biosensor (data not shown). At the concentration of 125 μg/mL R3 biosensor inhibition was 44 % ± 4.5 and at a concentration of 62.5 μg/mL R3 inhibition was 23 % ± 3.6 (data not shown). These data indicate that compounds exhibited dose-dependent selectivity toward QS signaling pathways and the highest tested concentration (250 μg/mL) of compounds showed PQS inhibitory activity (41–43% compound **2**, and 50–52 % compound **6**, Table 1.) suggesting that these compounds have a potential effect on pyocyanin production, too. Also, what can be observed is that the compounds that show a PQS inhibitory activity (**2** and **6**) contain as a chromophore one fragment of cinnamic acid with a methoxy group, in comparison to compound **4** that possesses two cinnamic acid fragments with a methoxy group, which suggests that the size of the molecules has an important influence on its antimicrobial activity (Scheme 1, Table 1). Compounds **2** and **6** had a five to six times stronger PQS inhibitor activity in comparison to compound **4** (Table 1). These results are consistent with the previously published in-silico analysis which revealed that cinnamic acid can act as a competitive inhibitor towards the ligand binding domain of the transcriptional activators of the quorum sensing circuit in *P. aeruginosa*, LasR, and RhlR [56,57].

Table 1
Percent of activity inhibition of *P. aeruginosa* QS biosensor strains in the presence of 250 μg/mL of novel PET derivatives.

Compound	R3	RHL	ΔPQS
1	23 ± 1.3	22 ± 2.1	20 ± 2.1
2	**35 ± 1.5**	**42 ± 0.1**	**43 ± 1.7**
3	NA	8.5 ± 0.5	25 ± 0.9
4	**22 ± 4.1**	**25 ± 1.0**	**9 ± 3.4**
5	28 ± 7.0	18 ± 2.4	35 ± 4.9
6	**41 ± 0.2**	**39 ± 2.2**	**52 ± 2.2**

NA = no activity.

3.3. Molecular docking studies

As we found that compounds **2** and **6** show effect on the QS pathway, more precisely, they inhibit the production of pyocyanin, we wanted to see if there is any specific interaction of these compounds with the most studied QS protein targets: LuxP (periplasmatic protein, that binds AI-2 inducer and forms a complex able to transduce the autoinducer signal) [28], AbaI (role in QS signal transduction) [58], LasR (which is a key QS transcriptional regulator that activates transcription of genes coding for some virulence-associated traits) [59], and RhlR (a key QS transcriptional regulator that activates the genes involved in the synthesis of rhamnolipids and pyocyanin) [59,60], and whether the size of the chromophore in the model compounds, as well as its functional groups, affect QS. Therefore, we performed molecular docking studies on the interactions of these proteins and our compounds, and the results of the calculations are shown in Table 2.

For the smaller PET model compounds **1** and **2**, both programs have found the highest binding energy with the LasR protein. This binding site is located in the autoinducer binding pocket of LasR protein [29] (Fig. 2**A**) and the main protein-ligand interactions include hydrogen bond between Arg 61 and the terephthalic carboxyl group, π−π stacking interactions between Tyr 64 and cinnamic acid aromatic ring and C—H−π interactions between Ala 50, Ala 70, and Val 76 and the terephthalic aromatic ring (Fig. 2**B** and **C**). To compare binding energies and docking poses, a redocking experiment [61,62] with LasR noncognate autoinducer 3-oxo-N- [(3S)-2-oxotetrahydrofuran-3-yl] decanamide, also termed as $3OC_{10}$ homoserine lactone ($3OC_{10}$HSL), found in the LasR crystal structure (PDBID: 6MVN [25]) was conducted. The results of the redocking experiment (**Fig. S2**), with the AutoDock4 program, have predicted a binding energy of −8.52 kcal/mol for $3OC_{10}$HSL to LasR. This binding energy is lower than predicted for PET model compounds **1** and **2** (−9.61 and −9.88 kcal.mol, Table 2) indicating the potential of these compounds to act as competitive inhibitors. Much larger PET model compounds (**3, 4,** and **6**) cannot fit in small autoinducer binding pockets, so the best binding pose for them is located at the surface of the LasR protein (Fig. 2**A**). Compound **5**, can just fit in the autoinducer binding pocket but in the highly bent conformation (**Fig. S3**) and with a high conformational penalty, significantly lowering total binding energy (−8.7 kcal/mol). This binding pose was only found with the AutoDock Vina program (**Fig. S4**).

The highest energy binding site for larger PET model compounds (**3, 4, 5,** and **6**) is found in the inhibitor binding domain of AbaI (Fig. 3**A**)

Table 2
Interaction of PET model compounds with the QS protein targets, expressed in kcal/mol, obtained by molecular docking analyses with AutoDock Vina program (upper part) and AutoDock4 program (lower part).

Compound / *Protein*	1	2	3	4	5	6
			AutoDock Vina			
LuxP	−9.2	−9.2	−9.2	−8.8	−9.2	−9.2
AbaI	−8.5	−8.4	**−9.8**	**−9.7**	**−9.6**	**−9.5**
LasR	**−10.1**	**−9.7**	−7.6	−7.6	−8.7	−7.3
RhlR	−8.8	−8.8	−8.4	−8.6	−8.8	−8.7
	AutoDock4					
LuxP	−9.14	−9.51	−9.15	−8.12	−10.0	−8.46
AbaI	−8.98	−9.27	**−11.00**	**−11.41**	**−10.12**	**−9.80**
LasR	**−9.61**	**−9.88**	−7.88	−8.19	−7.40	−7.39
RhlR	−8.44	−8.21	−8.57	−8.30	−8.51	−7.77

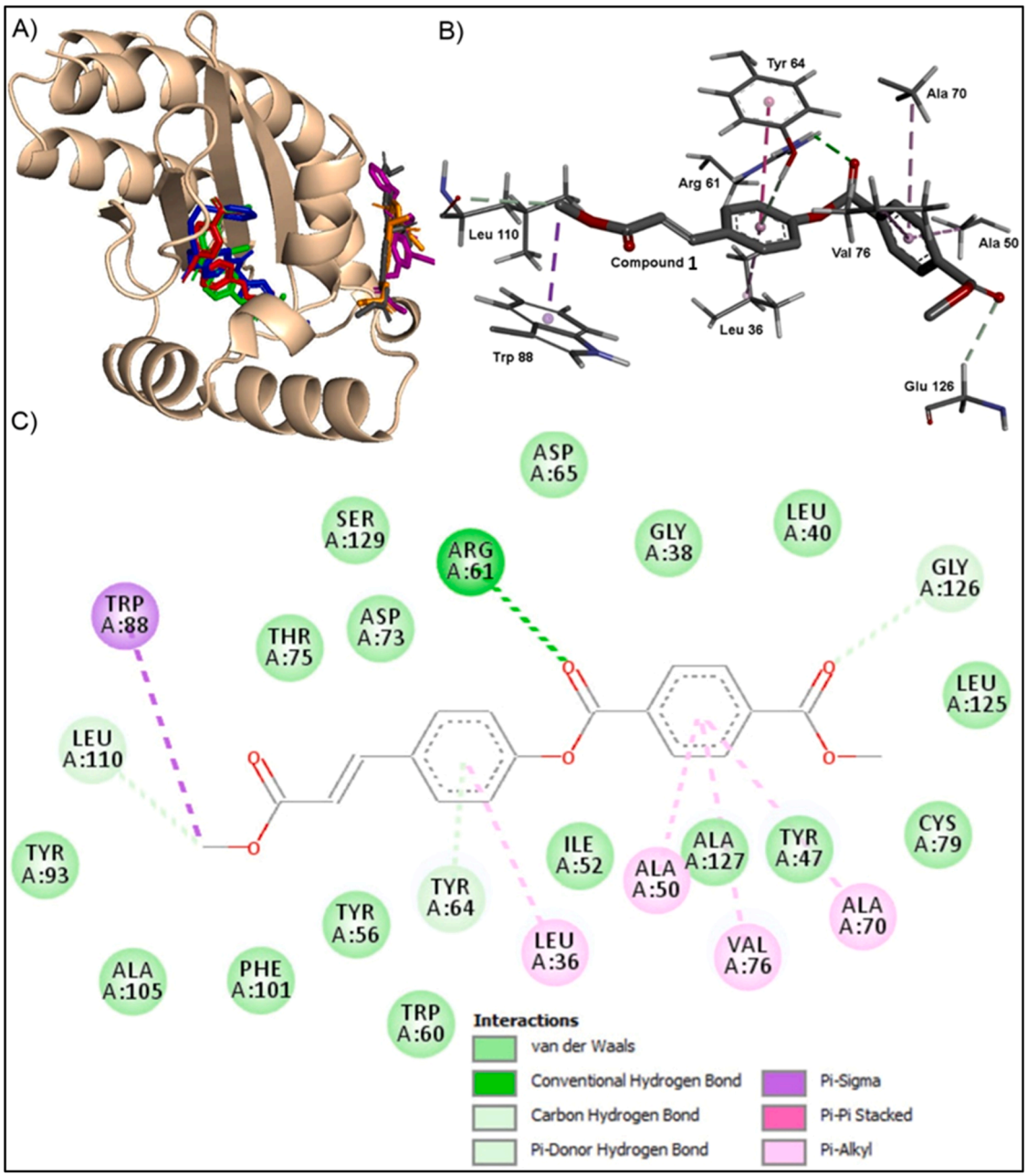

Fig. 2. **A**) High energy binding poses for PET model compound (stick representations) 1 (red), 2 (green), and 5 (blue) in autoinducer binding pocket of LasR protein. Compounds 3 (black), 4 (orange), and 6 (purple) are bound to the surface of the LasR protein. **B**) 3D and **C**) 2D interaction diagrams between the highest energy binding pose for compound **1** and LasR amino acids.

protein with calculated binding energies with AutoDock Vina software between −9.5 and −9.8 kcal/mol, and between −11.41 and −9.80 with AutoDock4 software. This binding site is also the target for binding potent QS inhibitor erythromycin, as found by a recent docking study [30]. Ligand binding in this site is dominated by aromatic–aromatic interactions, between Phe 83 and Trp 33 and aromatic rings from PET-modeled compounds (Fig. 3**B** and **C**). Smaller PET model compounds (**1** and **2**) will also bind in this binding site but with lower binding energy. To verify the validity of the found biding site two additional docking experiments on the AbaI protein with N-(3-oxocyclohex-1-en-1-yl)octanamide (J8-C8) and S-adenosyl methionine (SAM) were conducted. A previous study [63] has shown that J8-C8 can inhibit the binding of SAM to the Acyl-homoserine-lactone synthase protein TofI. A crystal structure of TofI with J8-C8 bound in the inhibitor-binding pocket was deposited in the Protein Data Bank (PDB ID:3P2H) and was used as a template for modeling AbaI protein. The docking experiment of J8-C8 to AbaI protein helped us identify an inhibitor-binding pocket and produced a binding site very similar to that found in the crystal structure of TofI, and almost completely overlaps with predicted PET model compounds binding site (Fig. 4). The highest binding energy of J8-C8 to AbaI was −7.82 kcal/mol predicted by the AutoDock4 program, and was significantly lower than predicted binding energies for all PET model compounds (from −11.41 to −8.98 kcal/mol, Table 2). Finally, docking of SAM (the natural ligand of AbaI and other Acyl-homoserine-lactone synthase) to the AbaI protein has shown a partial overlap between the inhibitor binding site and SAM binding site. More specifically, the methoxy group from ferulic acid in compounds **2, 4,** and **6** overlaps with the amino group from the methionine part of SAM (Fig. 4). This overlap can explain the increased inhibitor activity of ferulic acid PET derivates, compared to hydroxycinnamic acid PET

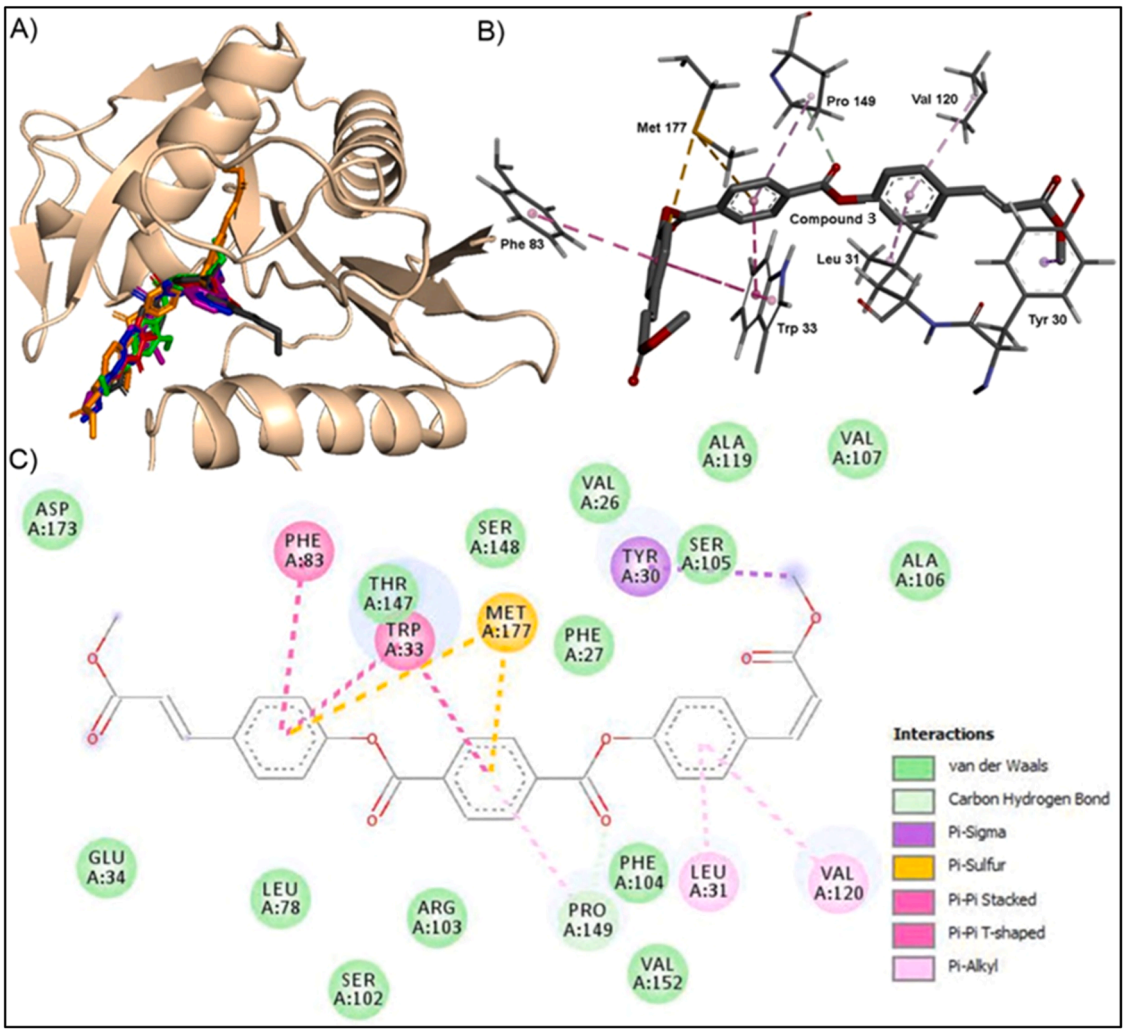

Fig. 3. **A)** High energy binding poses for PET model compounds (stick representations) in the ligand binding domain of AbaI protein. Color code: red – compound 1; green – compound 2; black – compound 3; orange – compound 4; blue – compound 5; purple – compound 6. **B**) 3D and **C**) 2D interaction diagrams between the highest energy binding pose for compound **3** and AbaI amino acids.

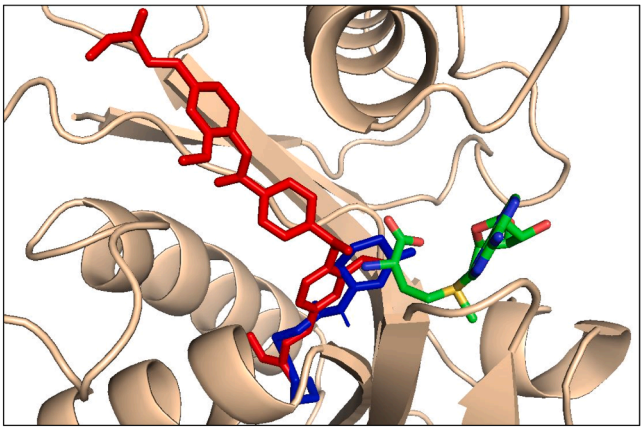

Fig. 4. J8-C8 inhibitor (blue) and PET model compound **4** (red) docked in the inhibitor binding site of AbaI protein. This binding site partially overlaps with the SAM (carbon – green, nitrogen – blue, oxygen – red, sulfur – yellow) binding site.

derivates (Table 1).

Docking studies, with both docking programs [64–70], on binding **1–6** PET model compounds to LuxP and RhlR proteins, produced two discreet binding pockets but with smaller binding energies than for LasR and AbaI (Table 2.). The results of these studies are shown in ESI. These results support our idea that PET model compounds having a single cinnamic acid moiety with a methoxy functional group act as quorum-sensing modulators.

4. Conclusion

The development of new antimicrobials is a huge challenge, the research and development process is time-consuming and expensive, and antimicrobial resistance is growing day by day. In the search for new pharmacologically active compounds against antimicrobial resistance, cinnamic acid-based derivatives are represented as valuable compounds with great potential for development into drugs. In this study, we synthesized labeled PET model compounds featuring chromophores in the form of cinnamic and ferulic acid derivatives. These compounds were subjected to a systematic screening process, including solubility studies, biological activity studies, and molecular docking studies, marking the first time such investigations were conducted. Even though compounds showed no effects on microbial growth, we discovered their potential in the inhibition of microbial communication, i.e., quorum-sensing, where

it was determined that compounds with one cinnamic acid fragment with methoxy group (compounds **2** and **6**) have an impact on bacterial communication. Further on, molecular docking studies have shown that the compounds possess the power of interaction, i.e. binding to all four QS protein targets, indicating that molecules with a more complex structure (larger molecules **3, 4, 5, 6**) favor interaction with the AbaI protein, while smaller molecules (**1, 2**) interact with the LasR protein. Moreover, through the molecular docking studies, we found that the methoxy group from ferulic acid in compounds **2, 4,** and **6** increased the inhibitor activity of ferulic acid PET derivates, compared to hydroxycinnamic acid PET derivates.

Altogether, our data show that the incorporation of cinnamic acid into PET polymer are potential candidate to be utilized in a reduction of PET bacterial contamination, and further structure modifications would be beneficial to endow them with a better antibacterial effect.

Research ethics

We further confirm that any aspect of the work covered in this manuscript that has involved human patients has been conducted with the ethical approval of all relevant bodies and that such approvals are acknowledged within the manuscript.

IRB approval was obtained (required for studies and series of 3 or more cases)

Written consent to publish potentially identifying information, such as details or the case and photographs, was obtained from the patient(s) or their legal guardian(s).

Our work did not involve human patients.

Funding

No funding was received for this work.

Supplementary material associated with this article can be found, in the online version, at _

CRediT authorship contribution statement

S Skaro Bogojevic: Conceptualization, Supervision, Writing – original draft. **D Perminova:** Investigation. **J Jaksic:** Investigation, Methodology. **M Milcic:** Conceptualization, Investigation. **V Medakovic:** Methodology. **J Milovanovic:** Investigation. **J Nikodinovic-Runic:** Conceptualization, Methodology, Visualization, Writing – original draft, Supervision. **V Maslak:** Conceptualization, Writing – original draft, Writing – review & editing, Supervision.

Declaration of Competing Interest

The authors declare that there are no competing financial and personal relationships with other people or organizations that could inappropriately influence (bias) their work. The authors declared no potential conflicts of interest.

Data availability

Data will be made available on request.

Acknowledgments

The authors gratefully acknowledge the financial support provided by the Ministry of Education, Science and Technological Development of the Republic of Serbia, 451-03-47/2023-01/ 200042, and the European Union's Horizon 2020 Research and Innovation Programme under grant agreement No. 870292 (BioICEP).

Supplementary materials

Supplementary material associated with this article can be found, in the online version, at doi:10.1016/j.molstruc.2023.137291.

References

[1] T. Çaykara, et al., Exploring the potential of polyethylene terephthalate in the design of antibacterial surfaces, Med. Microbiol. Immunol. 209 (3) (2020) 363–372.
[2] C. Adlhart, et al., Surface modifications for antimicrobial effects in the healthcare setting: a critical overview, J. Hosp. Infect. 99 (3) (2018) 239–249.
[3] M. Benkocká, et al., Antimicrobial and optical properties of PET chemically modified and grafted with borane compounds, RSC Adv. 8 (27) (2018) 15001–15008.
[4] K. Szafran, et al., Surface properties of the polyethylene terephthalate (PET) substrate modified with the phospholipid-polypeptide-antioxidant films: design of functional biocoatings, Pharmaceutics 14 (12) (2022) 2815.
[5] M. Alidadykhah, et al., Functionalization and modification of polyethylene terephthalate polymer by AgCl nanoparticles under ultrasound irradiation as bactericidal, ACS Omega 7 (23) (2022) 19141–19151.
[6] J. Li, et al., Anti-bacterial properties of ultrafiltration membrane modified by graphene oxide with nano-silver particles, J. Colloid Interface Sci. 484 (2016) 107–115.
[7] H. Gappa-Fahlenkamp, R.S. Lewis, Improved hemocompatibility of poly(ethylene terephthalate) modified with various thiol-containing groups, Biomaterials 26 (17) (2005) 3479–3485.
[8] J. Moncada, M.D. Dadmun, The structural evolution of poly(ethylene terephthalate) oligomers produced via glycolysis depolymerization, J. Mater. Chem. A 11 (9) (2023) 4679–4690.
[9] M. Djapovic, et al., Synthesis and characterization of polyethylene terephthalate (PET) precursors and potential degradation products: toxicity study and application in discovery of novel PETases, Chemosphere 275 (2021), 130005.
[10] H.R. El-Seedi, et al., Biosynthesis, natural sources, dietary intake, pharmacokinetic properties, and biological activities of hydroxycinnamic acids, J. Agric. Food Chem. 60 (44) (2012) 10877–10895.
[11] N. Ruwizhi, B.A. Aderibigbe, Cinnamic acid derivatives and their biological efficacy, Int. J. Mol. Sci. 21 (16) (2020) 5712.
[12] K. Gryko, et al., Natural cinnamic acid derivatives: a comprehensive study on structural, anti/pro-oxidant, and environmental impacts, Materials (Basel) 14 (20) (2021) 6098.
[13] A.C. Fonseca, et al., Cinnamic acid derivatives as promising building blocks for advanced polymers: synthesis, properties and applications, Polym. Chem. 10 (14) (2019) 1696–1723.
[14] T. Hoeks, et al., Synthesis and characterization of photo-crosslinkable copoly (carbonate-ester)s (PCE) derived from p-Hydroxy cinnamic acid (p-HCA) and bisphenol A (BPA), J. Macromol. Sci., Part A 56 (8) (2019) 812–820.
[15] B. Kaczmarek-Szczepańska, S. Grabska-Zielińska, M. Michalska-Sionkowska, The application of phenolic acids in the obtainment of packaging materials based on polymers—a review, Foods 12 (2023), https://doi.org/10.3390/foods12061343.
[16] N. Ruwizhi, B.A. Aderibigbe, Cinnamic acid derivatives and their biological efficacy, Int. J. Mol. Sci. 21 (2020), https://doi.org/10.3390/ijms21165712.
[17] A. Gunia-Krzyżak, et al., Cinnamic acid derivatives in cosmetics: current use and future prospects, Int. J. Cosmet. Sci. 40 (4) (2018) 356–366.
[18] R. Ordoñez, L. Atarés, A. Chiralt, Physicochemical and antimicrobial properties of cassava starch films with ferulic or cinnamic acid, LWT 144 (2021), 111242.
[19] R. Ordoñez, L. Atarés, A. Chiralt, Effect of ferulic and cinnamic acids on the functional and antimicrobial properties in thermo-processed PLA films, Food Packag. Shelf Life 33 (2022), 100882.
[20] J. Andrade, C. González-Martínez, A. Chiralt, Physical and active properties of poly (vinyl alcohol) films with phenolic acids as affected by the processing method, Food Packag. Shelf Life 33 (2022), 100855.
[21] N. Ruwizhi, B.A. Aderibigbe, Cinnamic acid derivatives and their biological efficacy, Int. J. Mol. Sci. 21 (16) (2020) 5712.
[22] M. Sova, Antioxidant and antimicrobial activities of cinnamic acid derivatives, Mini Rev. Med. Chem. 12 (8) (2012) 749–767.
[23] J.D. Guzman, Natural cinnamic acids, synthetic derivatives and hybrids with antimicrobial activity, Molecules 19 (2014) 19292–19349.
[24] M. Mingoia, et al., Synthesis and biological evaluation of novel cinnamic acid-based antimicrobials, Pharmaceuticals 15 (2) (2022) 228.
[25] F. Massai, et al., A multitask biosensor for micro-volumetric detection of N-3-oxo-dodecanoyl-homoserine lactone quorum sensing signal, Biosens. Bioelectron. 26 (8) (2011) 3444–3449.
[26] K. Duan, M.G. Surette, Environmental regulation of Pseudomonas aeruginosa PAO1 Las and Rhl quorum-sensing systems, J. Bacteriol. 189 (13) (2007) 4827–4836.
[27] M.P. Fletcher, et al., A dual biosensor for 2-alkyl-4-quinolone quorum-sensing signal molecules, Environ. Microbiol. 9 (11) (2007) 2683–2693.
[28] X. Chen, et al., Structural identification of a bacterial quorum-sensing signal containing boron, Nature 415 (6871) (2002) 545–549.
[29] A.R. McCready, et al., Structural determinants driving homoserine lactone ligand selection in the Pseudomonas aeruginosa LasR quorum-sensing receptor, Proc. Natl. Acad. Sci. U.S.A. 116 (1) (2019) 245–254.

[30] N.M. Seleem, et al., Drugs with new lease of life as quorum sensing inhibitors: for combating MDR Acinetobacter baumannii infections, Eur. J. Clin. Microbiol. Infect. Dis. 39 (9) (2020) 1687–1702.
[31] S. Nam, et al., Discovery and characterization of pure RhlR Antagonists against Pseudomonas aeruginosa Infections, J. Med. Chem. 63 (15) (2020) 8388–8407.
[32] R.A. Laskowski, et al., PROCHECK: a program to check the stereochemical quality of protein structures, J. Appl. Crystallogr. 26 (2) (1993) 283–291.
[33] G. Studer, et al., QMEANDisCo—distance constraints applied on model quality estimation, Bioinformatics 36 (6) (2020) 1765–1771.
[34] M. Wiederstein, M.J. Sippl, ProSA-web: interactive web service for the recognition of errors in three-dimensional structures of proteins, Nucleic Acids Res. 35 (suppl_2) (2007) W407–W410.
[35] C. Colovos, T.O. Yeates, Verification of protein structures: patterns of nonbonded atomic interactions, Protein Sci. 2 (9) (1993) 1511–1519.
[36] R. Kumari, et al., Structural-based virtual screening and identification of novel potent antimicrobial compounds against YsxC of Staphylococcus aureus, J. Mol. Struct. 1255 (2022), 132476.
[37] R. Anandakrishnan, B. Aguilar, A.V. Onufriev, H++ 3.0: automating pK prediction and the preparation of biomolecular structures for atomistic molecular modeling and simulations, Nucleic. Acids Res. 40 (Web Server issue) (2012) W537–W541.
[38] J. Huang, et al., CHARMM36m: an improved force field for folded and intrinsically disordered proteins, Nat. Methods 14 (1) (2017) 71–73.
[39] V. Dalal, R. Kumari, Screening and identification of natural product-like compounds as potential antibacterial agents targeting FemC of *Staphylococcus aureus*: an in-silico approach, ChemistrySelect 7 (42) (2022), e202201728.
[40] G.M. Morris, et al., AutoDock4 and AutoDockTools4: automated docking with selective receptor flexibility, J. Comput. Chem. 30 (16) (2009) 2785–2791.
[41] Becke, A.D., Density-functional thermochemistry. III. The role of exact exchange. 1993. 98: p. 5648–5652.
[42] C. Lee, W. Yang, R.G. Parr, Development of the Colle-Salvetti correlation-energy formula into a functional of the electron density, Phys. Rev. B Condens. Matter 37 (2) (1988) 785–789.
[43] Gaussian 09, R.D., M.J. Frisch, G.W. Trucks, H.B. Schlegel, G.E. Scuseria, M.A. Robb, J.R. Cheeseman, G. Scalmani, V. Barone, B. Mennucci, G.A. Petersson, H. Nakatsuji, M. Caricato, X. Li, H.P. Hratchian, A.F. Izmaylov, J. Bloino, G. Zheng, J. L. Sonnenberg, M. Hada, M. Ehara, K. Toyota, R. Fukuda, J. Hasegawa, M. Ishida, T. Nakajima, Y. Honda, O. Kitao, H. Nakai, T. Vreven, J.A. Montgomery, Jr., J.E. Peralta, F. Ogliaro, M. Bearpark, J.J. Heyd, E. Brothers, K.N. Kudin, V.N. Staroverov, T. Keith, R. Kobayashi, J. Normand, K. Raghavachari, A. Rendell, J.C. Burant, S.S. Iyengar, J. Tomasi, M. Cossi, N. Rega, J.M. Millam, M. Klene, J.E. Knox, J.B. Cross, V. Bakken, C. Adamo, J. Jaramillo, R. Gomperts, R.E. Stratmann, O. Yazyev, A.J. Austin, R. Cammi, C. Pomelli, J.W. Ochterski, R.L. Martin, K. Morokuma, V.G. Zakrzewski, G.A. Voth, P. Salvador, J.J. Dannenberg, S. Dapprich, A.D. Daniels, O. Farkas, J.B. Foresman, J.V. Ortiz, J. Cioslowski, and D.J. Fox, Gaussian, Inc., Wallingford CT, 2013.
[44] G.M. Morris, et al., AutoDock4 and AutoDockTools4: automated docking with selective receptor flexibility, J. Comput. Chem. 30 (16) (2009) 2785–2791.
[45] O. Trott, A.J. Olson, AutoDock Vina: improving the speed and accuracy of docking with a new scoring function, efficient optimization, and multithreading, J. Comput. Chem. 31 (2) (2010) 455–461.
[46] M. Šunderić, et al., Antipsychotic clozapine binding to alpha-2-macroglobulin protects interacting partners against oxidation and preserves the anti-proteinase activity of the protein, Int. J. Biol. Macromol. 183 (2021) 502–512.
[47] S. Minic, et al., Characterization and effects of binding of food-derived bioactive phycocyanobilin to bovine serum albumin, Food Chem. 239 (2018) 1090–1099.
[48] Dassault Systèmes BIOVIA, D.S.M.E., Release 2017, 2016.
[49] S.T. Nguyen, P.R.D. Murray, R.R. Knowles, Light-driven depolymerization of native lignin enabled by proton-coupled electron transfer, ACS Catal. 10 (1) (2020) 800–805.
[50] J. Malheiro, et al., Phytochemical profiling as a solution to palliate disinfectant limitations, Biofouling 32 (9) (2016) 1007–1016.
[51] J.F. Malheiro, et al., Evaluation of cinnamaldehyde and cinnamic acid derivatives in microbial growth control, Int. Biodeterior. Biodegrad. 141 (2019) 71–78.
[52] H.Z. Asfour, Anti-Quorum Sensing Natural Compounds, J. Microsc. Ultrastruct. 6 (1) (2018) 1–10.
[53] K.H. McClean, et al., Quorum sensing and Chromobacterium violaceum: exploitation of violacein production and inhibition for the detection of N-acylhomoserine lactones, Microbiology (Reading) 143 (Pt 12) (1997) 3703–3711.
[54] R. Van Houdt, M. Givskov, C.W. Michiels, Quorum sensing in Serratia, FEMS Microbiol. Rev. 31 (4) (2007) 407–424.
[55] P. Jantaruk, et al., 4-methoxybenzalacetone, the cinnamic acid analog as a potential quorum sensing inhibitor against Chromobacterium violaceum and Pseudomonas aeruginosa, World J. Microbiol. Biotechnol. 37 (9) (2021) 153.
[56] J. Rajkumari, et al., Cinnamic acid attenuates quorum sensing associated virulence factors and biofilm formation in Pseudomonas aeruginosa PAO1, Biotechnol. Lett. 40 (7) (2018) 1087–1100.
[57] T. Dua, et al., Novel Vanillin-based hybrids inhibit quorum sensing and silences phenotypical expressions in *Pseudomonas aeruginosa*, Drug Dev. Res. 84 (1) (2023) 45–61.
[58] X. Sun, et al., The abaI/abaR quorum sensing system effects on pathogenicity in Acinetobacter baumannii, Front. Microbiol. 12 (1791) (2021), 679241.
[59] E. Morales, et al., Pseudomonas aeruginosa quorum-sensing response in the absence of functional LasR and LasI proteins: the case of strain 148, a virulent dolphin isolate, FEMS Microbiol. Lett. 364 (12) (2017) fnx119.
[60] I.R. Taylor, et al., Inhibitor mimetic mutations in the pseudomonas aeruginosa PqsE enzyme reveal a protein–protein interaction with the quorum-sensing receptor RhlR that is vital for virulence factor production, ACS Chem. Biol. 16 (4) (2021) 740–752.
[61] R. Kumari, V. Dalal, Identification of potential inhibitors for LLM of Staphylococcus aureus: structure-based pharmacophore modeling, molecular dynamics, and binding free energy studies, J.Biomol. Struct. Dyn. 40 (20) (2022) 9833–9847.
[62] R. Kumari, P. Dhankhar, V. Dalal, Structure-based mimicking of hydroxylated biphenyl congeners (OHPCBs) for human transthyretin, an important enzyme of thyroid hormone system, J. Mol. Graph. Model. 105 (2021), 107870.
[63] J. Chung, et al., Small-molecule inhibitor binding to an N-acyl-homoserine lactone synthase, Proc. Natl. Acad. Sci. 108 (29) (2011) 12089–12094.
[64] L. Momeni, S. Farhadian, B. Shareghi, Study on the interaction of ethylene glycol with trypsin: binding ability, activity, and stability, J. Mol. Liq. 350 (2022), 118542.
[65] N. Dehdasht-Heidari, et al., Investigation on the interaction behavior between safranal and pepsin by spectral and MD simulation studies, J. Mol. Liq. 344 (2021), 117903.
[66] S. Sadeghi-kaji, et al., Investigation on the structure and function of porcine pancreatic elastase (PPE) under the influence of putrescine: a spectroscopy and molecular simulation study, J. Mol. Liq. 289 (2019), 111115.
[67] S. Sadeghi-Kaji, et al., Spermine as a porcine pancreatic elastase activator: spectroscopic and molecular simulation studies, J. Biomol. Struct. Dyn. 38 (1) (2020) 78–88.
[68] F. Yazdani, et al., Structural insights into the binding behavior of flavonoids naringenin with Human Serum Albumin, J. Mol. Liq. 349 (2022), 118431.
[69] S. Habibian Dehkordi, S. Farhadian, M. Ghasemi, The interaction between the azo dye tartrazine and α-Chymotrypsin enzyme: molecular dynamics simulation and multi-spectroscopic investigations, J. Mol. Liq. 344 (2021), 117931.
[70] Z. Asemi-Esfahani, et al., Food additive dye–lysozyme complexation: determination of binding constants and binding sites by fluorescence spectroscopy and modeling methods, J. Mol. Liq. 363 (2022), 119749.